ELSEVIER

PII: S0032-3861(97)00394-7

Polymer Vol. 39 No. 5, pp. 1197–1205, 1998

0032-3861/97/$17.00+0.00

Synthesis, thermal characterization and rheological properties of a homologous series of polymethacrylate-based side-chain liquid crystal polymers

Aileen A. Craig[a], Ian Winchester[a], Patricia C. Madden[a], Paul Larcey[b], Ian W. Hamley[c] and Corrie T. Imrie[a,*]

[a]*Department of Chemistry, University of Aberdeen, Meston Walk, Aberdeen AB24 3UE, UK*

[b]*Rheometric Scientific Ltd, Surrey Business Park, Weston Road, Kiln Lane, Epsom KT17 1JF, UK*

[c]*School of Chemistry, University of Leeds, Leeds LS2 9JT, UK*

(Revised 24 April 1997)

A new homologous series of side-chain liquid crystal polymers, the poly[ω-(4-cyanoazobenzene-4′-oxy)alkyl methacrylate]s, have been prepared in which the length of the flexible alkyl spacer is varied from 3 to 12 methylene units. All the polymers exhibit liquid crystalline behaviour; specifically, crystal E, smectic A and nematic phases are observed. The glass transition temperatures decrease on increasing spacer length before reaching a limiting value at *ca.* 30°C. The clearing temperatures exhibit an odd–even effect on varying the length and parity of the spacer. This is attributed to the change in the average shape of the side chain as the parity of the spacer is varied. This rationalization also accounts for the observed alternation in the entropy change associated with the clearing transition. A weak relaxation is observed rheologically for several members of this polymer series at temperatures above their respective glass transition temperatures. This is attributed either to specific motions of the smectic layers or to 180° reorientational jumps of the long axis of the mesogenic unit about the polymer backbone.

(Keywords: side chain liquid crystal polymers; transitional behaviour; rheology)

INTRODUCTION

Side-chain liquid crystal polymers (SCLCP) continue to be the focus of considerable research activity. This arises not only as a result of the application potential of this class of materials in a range of advanced electro-optic technologies[1–3], but also because they present a demanding challenge to our understanding of self-assembly in molecular systems[4–6]. A SCLCP has three structural components: a polymer backbone, a semi-rigid anisometric or mesogenic group and connecting these, a flexible spacer. The spacer plays a critical role in determining the properties of the polymer by decoupling the opposing tendency of the liquid crystal groups to self-assemble from that of the polymer backbones to adopt random coil conformations. Consequently SCLCPs exhibit a unique duality of properties; specifically, a SCLCP shows the electro-optic characteristics of low molar mass liquid crystals, albeit on a much slower time scale, combined with polymeric properties, such as glassy behaviour. Much of the research centred on SCLCPs has focused on their liquid crystalline behaviour and empirical rules have been developed relating molecular structure to mesogenic properties[4–6]. By contrast, the polymeric characteristics of these materials have received much less attention and surprisingly there have been few studies of their rheological behaviour[7–13]. An understanding of rheology and how it varies with structure and phase type will clearly play an important role in the fabrication of new devices. Thus we have prepared and characterized the thermal and rheological behaviour of a new homologous series of SCLCPS, the poly[ω-(4-cyanoazobenzene-4′-oxy)alkyl methacrylate]s, **1**, in which the length of the alkyl spacer has been varied from 3 to 12 methylene units. The series is given the acronym AzoB-*n*, where *n* denotes the number of carbon atoms in the spacer and to our knowledge this represents only the third complete series of polymethacrylate-based SCLCPs[1,14]. These particular polymers are unlikely to have any direct application potential, but instead were chosen with the expectation of providing materials with a range of mesogenic behaviour with which to initiate a programme of research with the aim of relating rheological and liquid crystalline behaviour.

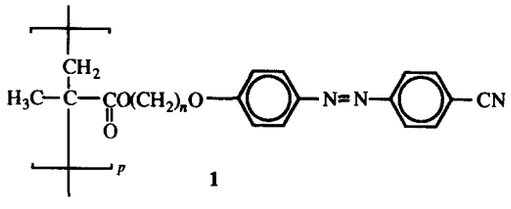

1

EXPERIMENTAL

The polymers were prepared using the synthetic route shown in *Scheme 1*. Identical experimental procedures were used to prepare all members of series **3** and **4** (see

* To whom correspondence should be addressed

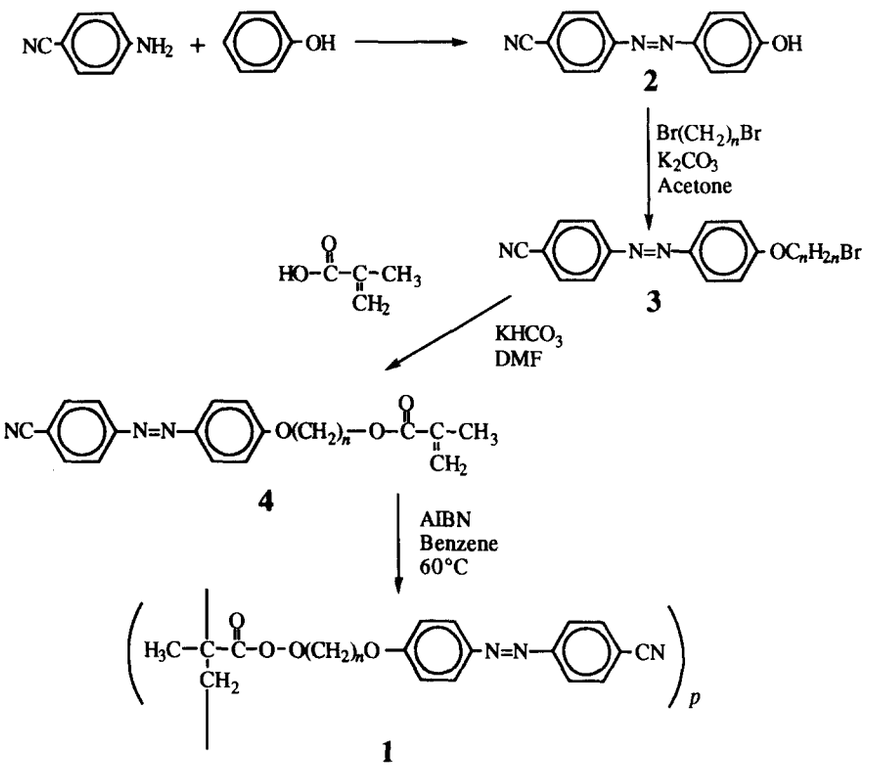

Scheme 1

Scheme 1), and hence only a representative description is given for the monomer synthesis.

Materials

α,ω-Dibromoalkanes (Aldrich) were distilled under reduced pressure using a Kugelrohr apparatus immediately prior to use. Benzene and tetrahydrofuran (THF) were distilled over calcium hydride. AIBN was purified by recrystallization from toluene, washed with petroleum spirits (80–100°C) and dried under vacuum. All other materials were used as received (Aldrich).

4-Hydroxy-4′-cyanoazobenzene (**2**) was prepared according to the method described by Stewart and Imrie[15]. Thus, 4-aminobenzonitrile (48.3 g, 0.409 mol) was dissolved in 3 M hydrochloric acid (500 ml) and the solution cooled in an ice/salt/water bath. A cooled solution of sodium nitrite (28.9 g, 0.419 mol) in distilled water (150 ml) was added slowly with vigorous stirring. The resulting diazonium salt solution was then slowly added to a stirred solution of phenol (39.4 g, 0.419 mol) in 10% aqueous sodium hydroxide (400 ml) at 0°C. After addition, the reaction mixture was allowed to stir for 30 min and then acidified. The resulting precipitate was collected by filtration, washed with copious amounts of water and dried under vacuum.

Yield: 59 g, 67%. MP: 171.4–172.7°C. Infrared (KBr)υ/cm^{-1}: 3043 (very strong OH), 2235 (very strong CN). ^{1}H NMR ($CDCl_3$)δ: 8.0 (m, 4H, aromatic), 7.8 (d, 2H, *J* 8.9 Hz, aromatic), 7.0 (d, 2H, *J* 8.9 Hz, aromatic), 1.6 (s, 1H, OH).

1-Bromo-5-(4′-cyanoazobenzene-4-oxy)pentane (**3**) was prepared using a procedure described by Attard *et al.*[16] Thus, **2** (3.6 g, 16.2 mmol), 1,5-dibromopentane (37.3 g, 162 mmol) and potassium carbonate (16.8 g, 121 mmol) were refluxed with stirring in dry acetone (250 ml) overnight. The reaction mixture was filtered hot, the residue washed with acetone, and the solvent removed under reduced pressure. Light petroleum (40–60°C) was added to the extract and the resulting precipitate collected. The crude product was recrystallized twice from ethanol with hot filtration to ensure the complete removal of any dimeric side-products.

Yield: 2.2 g, 37%. MP: 132.3–133.7°C. Infrared (KBr), υ/cm^{-1}: 2220 (very strong CN). ^{1}H NMR ($CDCl_3$)δ: 8.0 (m, 4H, aromatic), 7.8 (d, 2H, *J* 8.4 Hz, aromatic), 7.0 (d, 2H, *J* 8.9 Hz, aromatic), 4.1 (t, 2H, *J* 6.3 Hz, OCH_2), 3.4 (t, 2H, *J* 6.7 Hz, CH_2Br), 1.8–2.1 (m, 4H, $OCH_2\underline{CH_2}$, $\underline{CH_2}CH_2Br$), 1.6–1.8 (m, 2H, $O(CH_2)_2\underline{CH_2}(CH_2)_2Br$).

5-(4′-Cyanoazobenzene-4-oxy)pentyl methacerylate (**4**) was prepared using a modification of the procedure described by Nakano *et al.*[17] and Shannon[18]. Methacrylic acid (0.53 g, 6.2 mmol) was stirred with potassium hydrogen carbonate (0.61 g, 6.1 mmol) for 5 min at room temperature to form the potassium methacrylate salt. This salt was added to **3** (2.1 g, 5.6 mmol) and hydroquinone (0.0098 g, 0.09 mmol) in N,N′-dimethylforimamide (100 ml) and the reaction mixture was refluxed with stirring at 100°C overnight. On cooling, the mixture was poured into water (*ca.* 300 ml), the precipitate collected by filtration and dissolved in dichloromethane. The organic solution was washed with 5% aqueous NaOH and water. The organic layer was dried over $MgSO_4$ and the solvent removed. The crude product was recrystallized twice from ethanol.

Yield: 1.2 g, 57%. MP: 84.1–85.6°C. Infrared (KBr)υ/cm^{-1}: 2220 (very strong CN), 1714 (very strong C=O), 1637 (C=C). ^{1}H NMR ($CDCl_3$)δ: 8.0 (m, 4H, aromatic), 7.8 (d, 2H, *J* 8.6 Hz, aromatic), 7.0 (d, 2H, *J* 9.0 Hz, aromatic), 5.6, 6.1 (s, 2H, CH_2=C), 4.2 (t, 2H, *J* 6.5 Hz, $H_2COC(O)$), 4.0 (t, 2H, *J* 6.3 Hz, OCH_2),2.0 (s, 3H, CH_3) 1.7–2.0 (m,4H,$OCH_2\underline{CH_2}$, $\underline{CH_2}CH_2OC(O)$),1.5–1.7 (m, 2H, $O(CH_2)_2\underline{CH_2}(\overline{CH_2})_2\overline{OC(O)}$).

Table 1 Molecular weights, polydispersities (*PD*) and number average degrees of polymerization (*DP*) for the AzoB-*n* series, **1**

n	$\bar{M}_n$ (g mol^{-1})	$\bar{M}_w$ (g mol^{-1})	*PD*	*DP*
3	13500	23000	1.69	39
4	20400	31000	1.49	56
5	16600	29000	1.72	44
6	19100	32000	1.68	49
7	17800	32000	1.81	44
8	18400	33000	1.80	44
9	20200	38000	1.89	47
10	15600	34000	2.16	35
11	27600	51000	1.83	60
12	29000	50000	1.73	61

POLYMERIZATION

Monomer **4** (1 g) was dissolved in dry dimethylfortmamide (10 ml), and 3 mol% AIBN was added as initiator. The reaction mixture was flushed with argon for 20 min and placed in a water bath at 60°C to initiate polymerization. After 48 h the reaction was terminated on addition of THF (15 ml) and the polymer precipitated in a large amount of methanol. The polymer was then redissolved in chloroform and reprecipitated into methanol. This was repeated until the polymer contained no trace of monomer. The removal of the alkene was monitored spectroscopically; specifically, the alkene stretch at 1637 cm^{-1} in the i.r. spectra of the monomer and the peaks associated with the alkene protons at 5.6 and 6.1 ppm in the ^{1}H NMR spectra were not present in those of the corresponding polymer.

Yield: 0.67 g, 65%. Infrared (KBr) υ/cm^{-1}: 2226 (very strong CN), 1726 (very strong C=O). ^{1}H NMR ($CDCl_3$) δ: 7.8 (m, 4H, aromatic), 7.7 (m, 2H, aromatic), 6.9 (m, 2H, aromatic), 3.8–4.0 (m, 4H, OCH_2, $CH_2OC(O)$), 1.3–2.0 (m, 8H, CH_2), 0.8–1.2 (m, 3H, CH_3).

Characterization

The proposed structures of all the compounds were verified using ^{1}H NMR and i.r. spectroscopy. ^{1}H NMR spectra were measured in $CDCl_3$ or THF-d_8 on a Bruker AC-F 250 MHz NMR spectrometer. Infrared spectra were recorded using a Nicolet 205 FTIR spectrometer. The purities of all the intermediates were verified using thin layer chromatography. The molecular weights of the polymers were measured by gel permeation chromatography (GPC) using a Knauer Instruments chromatograph equipped with two PL gel 10 μm mixed columns and controlled by Polymer Laboratories GPC SEC V5.1 Software. THF was used as the eluent. A calibration curve was obtained using polystyrene standards.

The thermal properties of the polymers were determined by differential scanning calorimetry (DSC) using a Polymer Laboratories PL-DSC equipped with an autocool accessory and calibrated using an indium standard. Two samples were used for each polymer and the results averaged. The time–temperature profile for each was identical. Thus, each sample was heated from 25 to 220°C, maintained at 220°C for 3 min, cooled to −50°C, maintained at −50°C for 3 min, and finally reheated to 220°C. The heating and cooling rate in all cases was 10°C min^{-1}. Phase identification was performed by polarized light microscopy using an Olympus BH-2 optical microscope equipped with a Linkam THMS 600 heating stage and TMS 91 control unit. Clear, characteristic optical textures from which phase assignments were possible were obtained by cooling at either 0.2 or 0.1°C min^{-1} from *ca.* 10°C above the clearing temperature to below the glass transition temperature or, in the absence of glassy behaviour, to room temperature.

The mechanical behaviour of the polymers was investigated by dynamic mechanical thermal analysis (DMTA) using a PC-controlled Rheometric Scientific DMTA system comprising a 706 temperature programmer and a MkIII analyser. Experiments were performed over the temperature range 0–180°C using a ramping rate of 2°C min^{-1}. A frequency of 1 Hz was used for all measurements, and the shear mode was used to characterize the polymers. Samples were prepared by heating each polymer to the isotropic phase on a piece of Teflon tape, supported on a glass slide. The sample was compressed to uniform thickness using a second clean glass slide. This resulted in circular samples which were cut in half, and the Teflon tape removed from the underside. A slight compression force on the fixed plates of the clamps was necessary to locate the polymer correctly and to provide sufficient adhesion between the plates and the polymer.

The rheological behaviour of the polymers was investigated using a Rheometric Scientific Advanced Rheometric Expansion System (ARES) with 7.9 mm parallel plates. The samples were loaded at *ca.* 5°C above their clearing temperature and equilibrated for *ca.* 5 min. Frequency sweep (0.1–512 rad s^{-1}) measurements were performed for a range of temperatures and the strain was set at a fixed value corresponding to an amplitude of ± 1.0%.

RESULTS AND DISCUSSION

The molecular weights, polydispersities and average degrees of polymerization for the AzoB-*n* series, **1**, are

Table 2 Thermal properties of the AzoB-*n* series, **1**, extracted from the reheating DSC trace unless stated otherwise

n	T_g (°C)	T_{SS} (°C) T_{SN} (°C)*	T_{SI} (°C) T_{NI} (°C)*	ΔH_{SS} (kJ mol^{-1})	ΔH_{SI} (kJ mol^{-1}) ΔH_{NI} (kJ mol^{-1})*	$\Delta S_{SS}/R$	$\Delta S_{SI}/R$ $\Delta S_{NI}/R$*
3	88	—	147*	—	0.87*	—	0.25*
4	66	127*[a]	150*	—	0.63*	—	0.18*
5	55	—	169	—	2.09	—	0.57
6	40	67[b]	153	1.08[b]	1.67	0.38[b]	0.47
7	37	65[b]	167	1.55[b]	2.74	0.55[b]	0.75
8	33	63[b]	155	1.66[b]	2.37	0.59[b]	0.67
9	37	59[b]	159	1.40[b]	3.05	0.51[b]	0.85
10	30	50[b]	156	1.09[b]	3.43	0.40[b]	0.96
11	37	59[b]	159	2.62[b]	3.71	0.95[b]	1.03
12	33	58[b]	157	3.59[b]	3.90	1.31[b]	1.09

[a]Appears as a shoulder.
[b]Temperatures taken from the initial heat in the DSC trace.

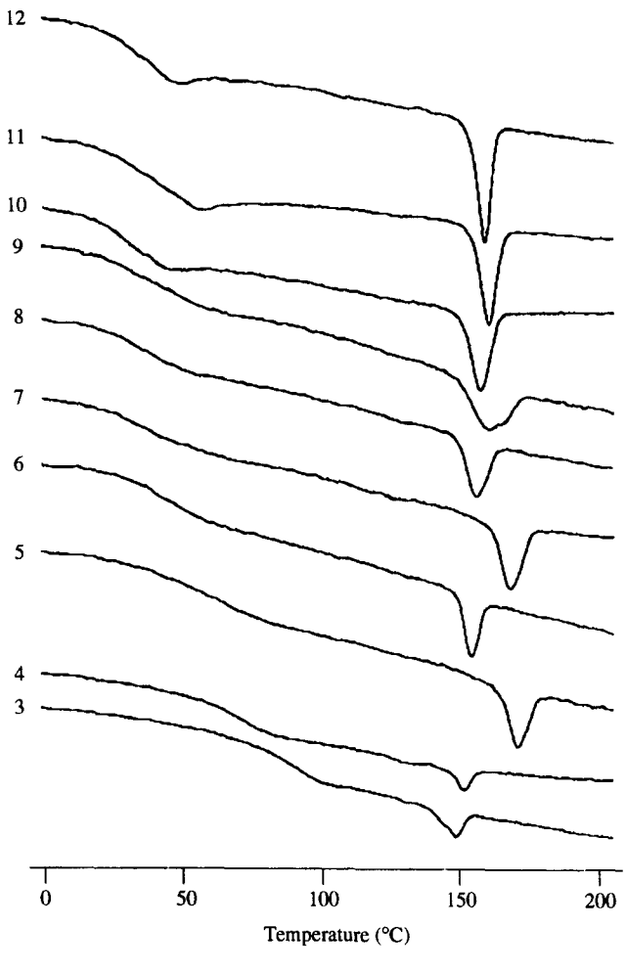

Figure 1 Normalized DSC traces obtained on the second heating of the AzoB-*n* series, **1**

listed in *Table 1*. The number average molecular weights of the polymers range from 13 500 to 29 000 g mol^{-1} with corresponding average degrees of polymerization in the range 36–55. These high molecular weights ensure that the thermal behaviour of the polymers do not lie within the molecular weight-dependent regime[19].

The thermal properties of the AzoB-*n* series are listed in *Table 2*. The clearing temperatures and associated enthalpy changes have been extracted from the second heating cycle of the DSC time–temperature profile, whereas the data for the lower temperature smectic–smectic transitions have been extracted from the initial heating trace. The normalized DSC reheating traces are shown in *Figure 1*.

In the DSC trace of the propyl homologue, i.e. AzoB-3, an endothermic peak associated with the clearing transition and a second-order transition are observed. The latter transition is assigned as a glass transition. On cooling the sample from the isotropic phase, a poorly defined Schlieren texture was obtained which was assigned as a nematic phase. The entropy change associated with the transition ($\Delta S/R = 0.25$) is consistent with this assignment. No further change in the optical texture was observed on cooling to room temperature. The DMTA trace for AzoB-3 (see *Figure 2*) shows a peak in the tan δ plot at 98°C, and presumably this is associated with the glass transition. A broad transition centred at 115°C is also observed; the molecular significance of this will be discussed later.

The DSC trace for AzoB-4 contains an endothermic peak with a small associated shoulder at *ca.* 127°C and a glass transition. Cooling from the isotropic phase produces a poorly defined nematic Schlieren texture similar to that observed for AzoB-3, and the clearing entropy ($\Delta S/R = 0.18$) is consistent with a nematic–isotropic transition. On further cooling to temperatures below that corresponding to the peak's shoulder, a poorly defined focal conic fan texture develops which is indicative of a smectic phase. The glass transition detected using DSC is not evident in the DMTA

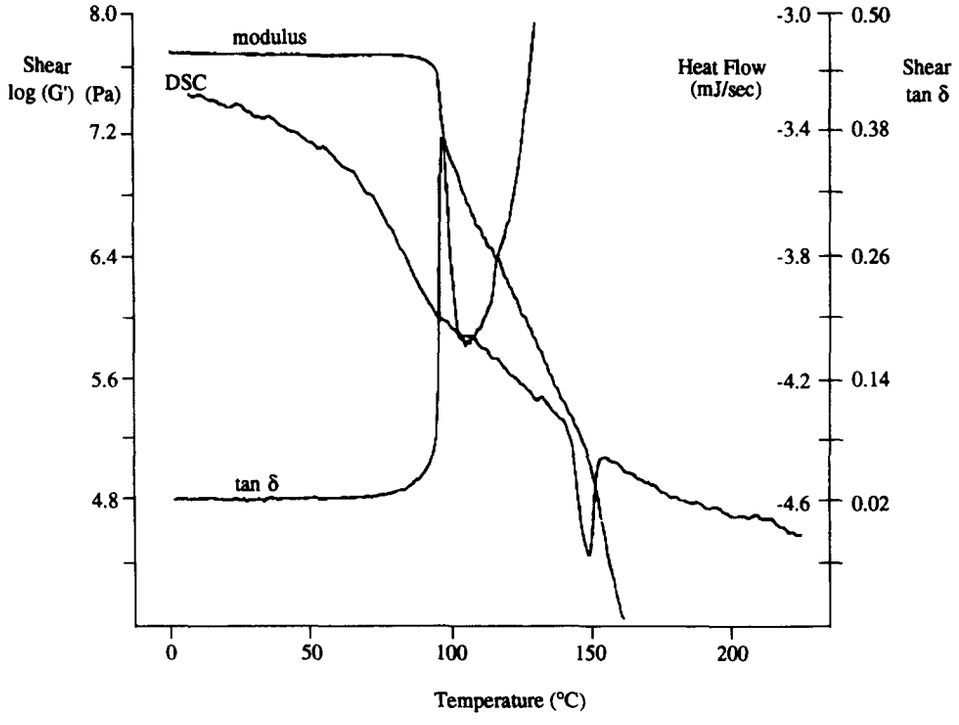

Figure 2 DSC and DMTA traces for AzoB-3

trace; instead, a gradual softening of the sample is observed together with a broad relaxation centred at *ca.* 110°C. The frequency sweeps for AzoB-3 and AzoB-4 also clearly show a phase transition between 90 and 100–110°C (see *Figure 3*), and we will return to this observation later.

The DSC trace for AzoB-5 shows an endothermic peak and a glass transition. On cooling from the isotropic phase, a well-defined focal conic fan texture develops and this is assigned as a smectic A phase. As for AzoB-3 and AzoB-4, a broad relaxation is observed at 118°C in the DMTA trace while there is no apparent change in the shear modulus indicative of a glass transition. The DSC traces obtained on reheating AzoB-6, AzoB-7, AzoB-8 and AzoB-9 all show a strong endothermic peak and a glass transition (see

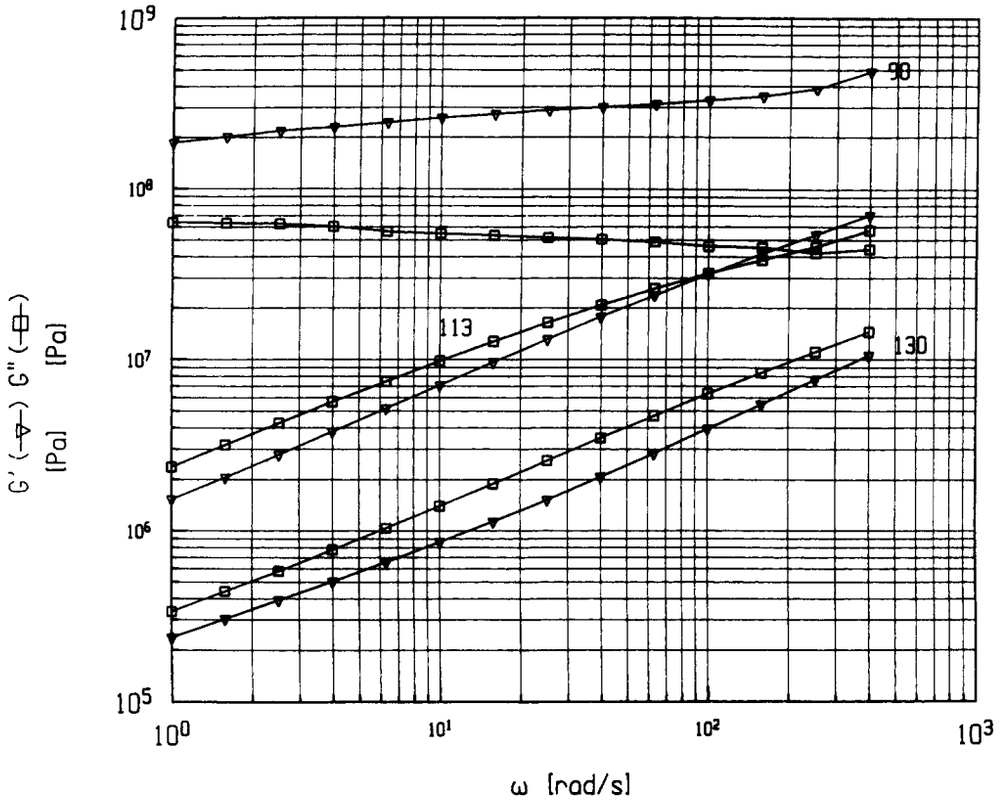

Figure 3 Dependence of the shear moduli on frequency for AzoB-3; the temperature (°C) is marked on each frequency sweep

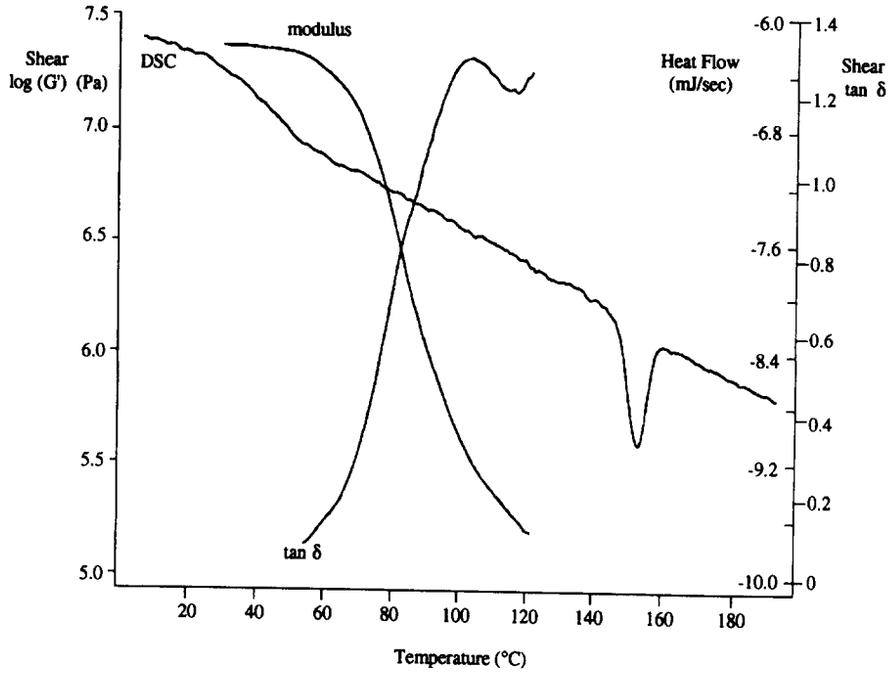

Figure 4 DSC and DMTA traces for AzoB-6

Figure 1). All these polymers, however, exhibit two endothermic peaks in the initial heating trace (see *Table 2*). On cooling these samples from the isotropic phase, all develop well-defined focal conic fan textures which are assigned as smectic A phases. Cooling to below the temperature associated with the lower temperature endotherm in the initial heating DSC trace produces bands across the backs of the fans which persist until room temperature. This is indicative of a crystal E–smectic A phase transition. The proximity of the glass transition presumably kinetically suppresses this phase transition in the DSC. The DMTA traces of AzoB-6 (see *Figure 4*), AzoB-7, AzoB-8 and AzoB-9 all show a broad relaxation centred in the range 90–115°C. This is also evident in the

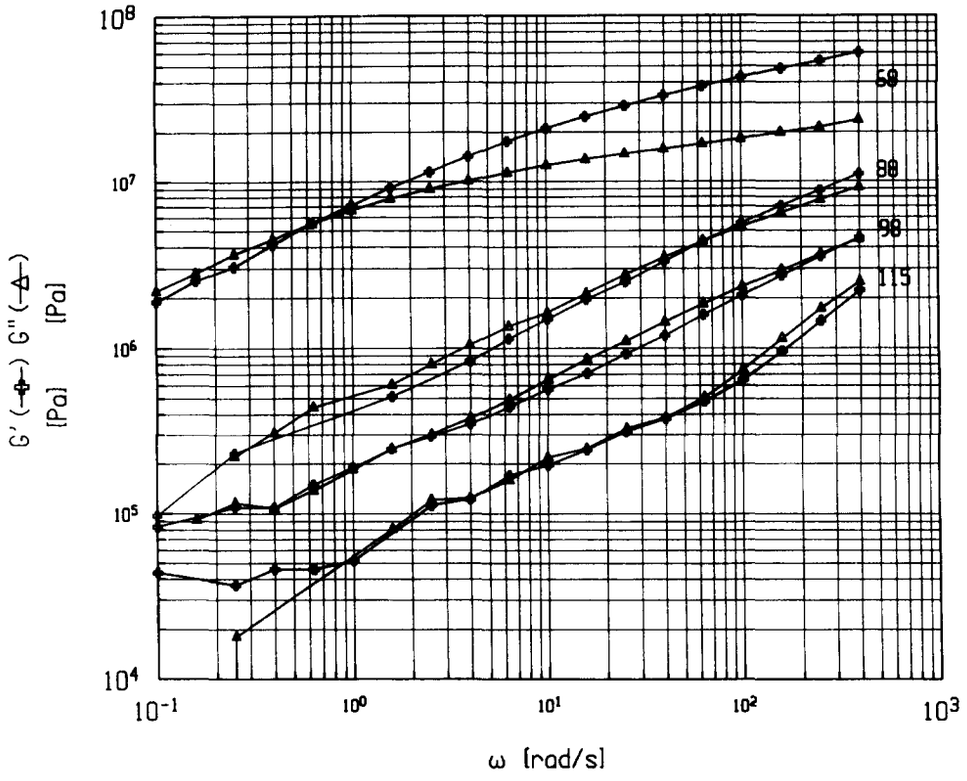

Figure 5 Dependence of the shear moduli on frequency for AzoB-6; the temperature (°C) is marked on each frequency sweep

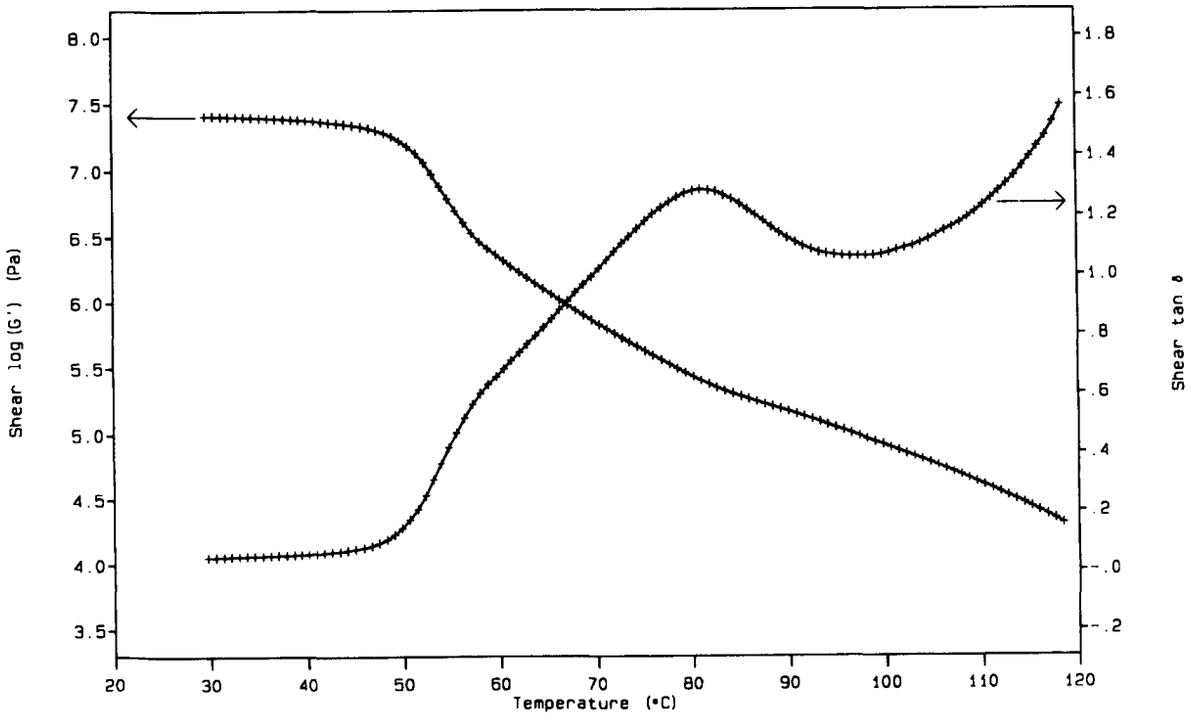

Figure 6 DMTA trace for AzoB-10

frequency sweep for AzoB-6 (see *Figure 5*). For AzoB-7, a small change in the shear modulus coincides with the E–S_A phase transition detected by DSC.

The DSC reheat traces for AzoB-10, AzoB-11 and AzoB-12 show a strong endothermic peak and a glass transition, but two endothermic peaks are observed in the initial heat. At the offset of the glass transition on reheating, however, a small peak can be seen (see *Figure 1*) which may be attributed to the lower temperature transition observed in the initial heat. All these samples show similar textures on cooling from the isotropic phase; thus, well-defined focal conic fans are produced and bands develop across their backs on cooling to temperatures below the lower temperature transition. As a consequence, the higher temperature phase is assigned as a smectic A phase and the lower temperature phase as an E phase. The DMTA traces for AzoB-10 and AzoB-12 exhibit two weak transitions evidenced by peaks in tan δ (see, for example, *Figure 6*) at *ca.* 40 and 80°C, and at *ca.* 55 and 76°C, respectively. The lower temperature relaxation is presumably associated with the glass transition. AzoB-11 shows a single weak relaxation in the DMTA trace at 76°C.

Figure 7 shows the dependence of the transition temperatures on varying the number of methylene units in the flexible alkyl spacer for the AzoB-*n* series. The glass transition temperatures initially decrease on increasing *n* before reaching a limiting value of *ca.* 30°C. This behaviour may be attributed to a plasticization of the polymer backbone by the side chains. The clearing temperatures exhibit an odd–even effect as the length and parity of the spacer is varied in which the odd members exhibit the higher values. This alternation is attenuated as the spacer length is increased. A similar dependence of the clearing temperature on the length and parity of the spacer has been observed for other homologous series of side-chain liquid crystal polymers and has been accounted for in terms of the average shape of the side chain as the parity of the spacer is varied and its effect on the relative orientations of the mesogenic groups[1,14]. Specifically, for an odd membered spacer in the all-*trans* conformation the mesogenic group lies orthogonal to the polymer backbone. In addition, there exists a number of conformations containing a single *gauche* defect which preserve this arrangement of the mesogenic groups. In these conformations the mesogenic groups lie coparallel and hence, the anisotropic interactions between them are maximized. This results in higher clearing temperatures. By comparison, for an even-membered spacer the mesogenic groups are constrained to lie at some angle with respect to the backbone not only for the all-*trans* conformation, but also for all conformations containing a single *gauche* defect. The anisotropic interactions between mesogenic groups attached to the backbone via an even membered spacer are, therefore, reduced in comparison to those between groups attached via an odd membered spacer and hence lower clearing temperatures are observed.

Furthermore, the anisotropic liquid crystalline environment preferentially selects those elongated conformers which maximize the interactions between the mesogenic groups. Thus, at the clearing transition this model predicts that there should be a greater change in the conformational component of the clearing entropy for an odd-membered spacer than for an even-membered spacer. The clearing entropies for the AzoB-*n* series do indeed exhibit an odd–even effect as the parity of the spacer is varied (see *Figure 8*). It must be remembered, however, that the entropy change associated with the smectic A-isotropic transition has three main components: orientational, translational and conformational. It is the subtle interplay of these contributions that determines the overall entropy change and this interpretation of the alternation in terms of solely the conformational component must, therefore, be treated with some degree of caution. The attenuation in the odd–even effect exhibited by both the clearing temperatures (see *Figure 7*), and the clearing entropies (see *Figure 8*) on increasing the spacer length reflects the increased number of conformations available to the spacer.

The clearing temperature of AzoB-3 is anomalously low (see *Figure 7*). For a closely related series, the poly[ω-(4-cyanobiphenyl-4′-oxy)alkyl methacrylate]s, **2**, the propyl member was not mesogenic whereas the remaining members of the series exhibited liquid crystalline behaviour. These observations suggest that for the propyl spacer the partial overlap of the mesogenic units responsible, in part, for the high clearing temperatures observed for cyano substituted mesogens is hindered. Hence, lower than expected clearing temperatures are observed.

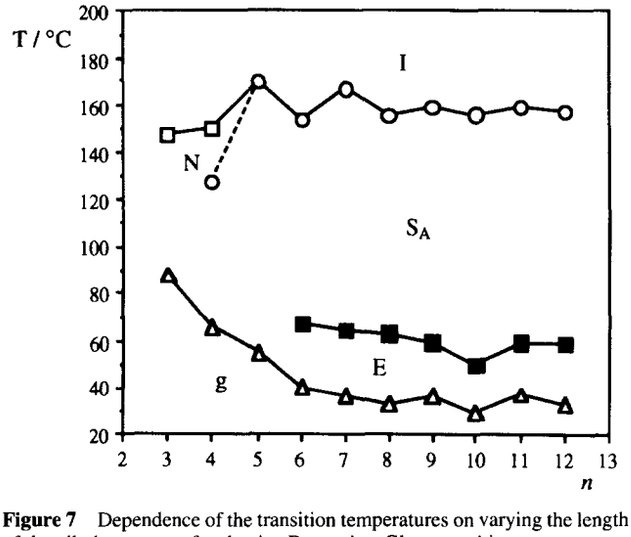

Figure 7 Dependence of the transition temperatures on varying the length of the alkyl spacer, *n*, for the AzoB-*n* series. Glass transition temperatures (△), smectic A-isotropic (○), nematic-isotropic (□) and E-smectic A (■)

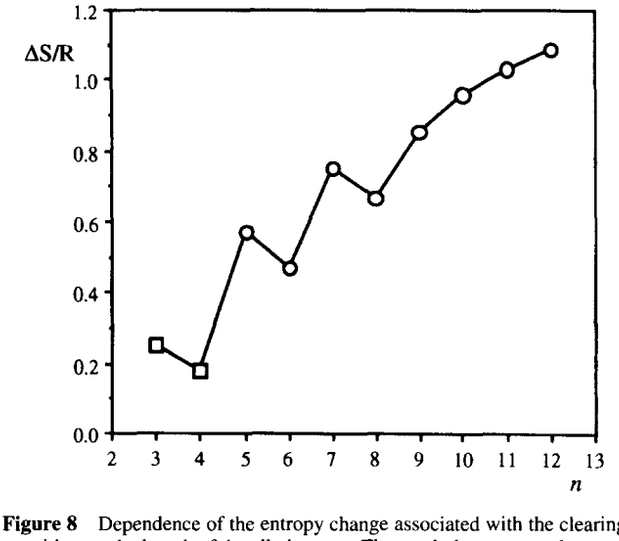

Figure 8 Dependence of the entropy change associated with the clearing transition on the length of the alkyl spacer. The symbols represent the same transitions as in *Figure 6*

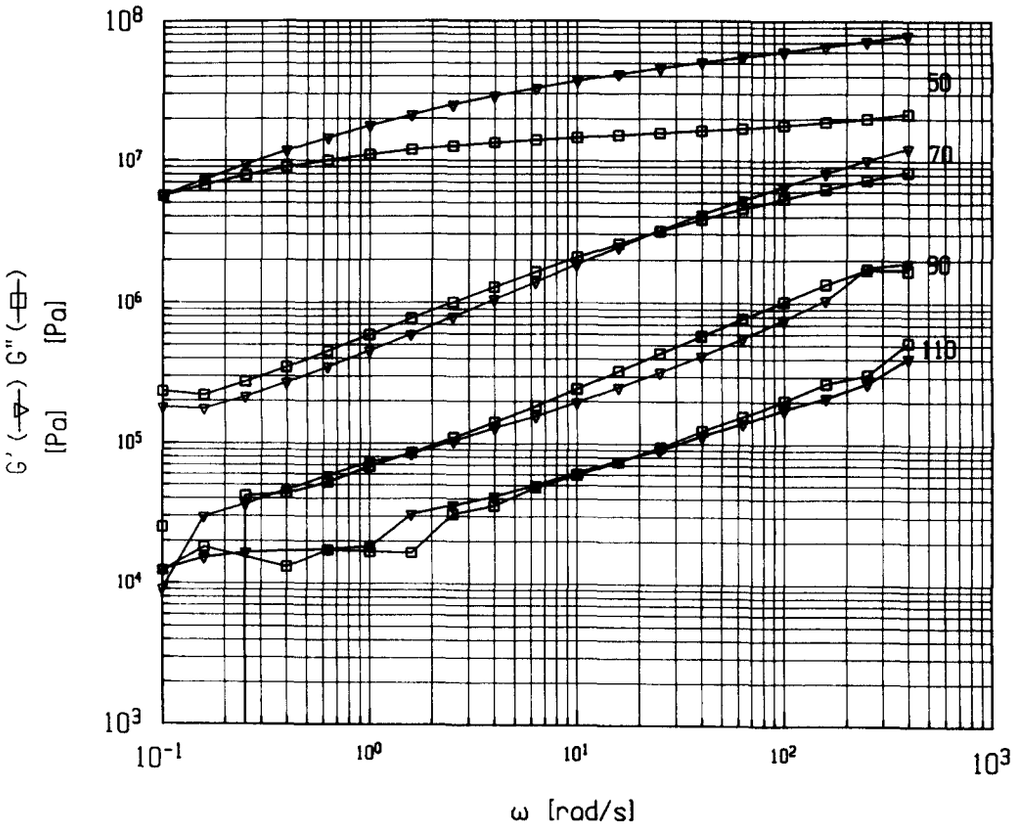

Figure 9 Dependence of the shear moduli on frequency for AzoB-10; the temperature (°C) is marked on each frequency sweep

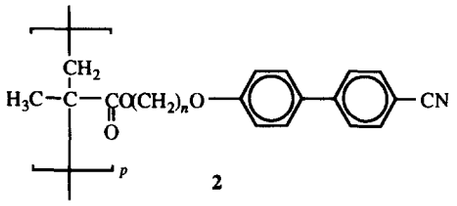

2

The characterization of the AzoB-*n* series using DMTA has yielded three unexpected observations. Firstly, with the exception of AzoB-3 and possibly also AzoB-10 and AzoB-12, the glass transitions detected using DSC for members of this series are not observed in their DMTA traces. This surprising result is in accordance with similar data reported for the poly[ω-(4-methoxybiphenyl-4′-oxy)alkyl methacrylate]s, **3**[13]. This suggests that the transition giving rise to a change in the specific heat capacity is such that the shear modulus is unchanged. It is possible, however, that the glass transition may be observed at a different shear rate because there is typically a frequency window within which it can be observed. Further speculation on this matter must now await detailed studies of a wider range of materials.

The second unexpected observation was the small change in the shear modulus accompanying the E–S_A transition; the frequency sweeps for AzoB-10 and AzoB-12 show that at 1 rad s^{-1} G' and G'' decease by *ca.* 1.5 orders of magnitude between 50 and 70°C (see *Figure 9*). By comparison, for series **3**, which are of comparable molecular weights, at the same transition the shear modulus decreased by *ca.* 3 orders of magnitude. It is possible, however, that the sample preparation quenched the S_A phase exhibited by the AzoB-*n* series.

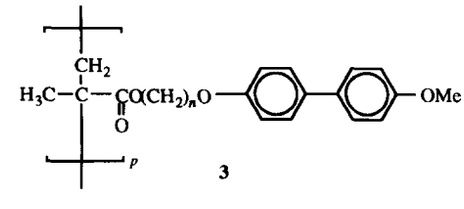

3

Finally, a weak relaxation is observed rheologically for several members of the AzoB-*n* series at temperatures considerably higher than the T_g detected using DSC. This relaxation may be related to specific motions of the smectic layers with respect to each other and thus may be considered analogous to the α_c-dispersion observed for crystalline polymers[20]. Alternatively, in order to interpret dielectric relaxation spectra obtained for polymethacrylate-based SCLCPs, Zentel *et al.*[21] attributed a relaxation occurring above T_g in a smectic phase to 180° reorientational jumps of the long axis of the mesogenic unit about the polymer backbone. The molecular origins of the broad relaxation observed for the AzoB-*n* series now requires further investigation.

REFERENCES

1. Bowry, C. and Bonnett, P., *Optical Computing Procedures*, 1981, **1**, 13.
2. Ikeda, T. and Tsutsumi, O., *Science*, 1995, **268**, 1873.
3. Blackwood, K. M., *Science*, 1996, **273**, 909.
4. Percec, V. and Pugh, C., in *Side Chain Liquid Crystal Polymers*, ed. C. B. McArdle. Blackie and Sons, Glasgow, 1989, Chap. 3.
5. Percec, V. and Tomazos, D., in *Comprehensive Polymer Science, First Supplement*, ed. S. L. Aggarwal and S. Russo. Pergamon, Oxford, 1992, Chap. 14.
6. Imrie, C. T., in *Polymeric Materials Encyclopedia*, ed. J. C. Salamone. 1996, Vol. 5, p. 3770.
7. Kannan, R. M., Kornfield, J. A., Schwenk, N. and Boeffel, C., *Macromolecules*, 1993, **26**, 2050.

8. Kannan, R. M., Rubin, S. F., Kornfield, J. A. and Boeffel, C., *Journal of Rheology*, 1994, **38**, 1609.
9. Colbly, R. H., Gillmore, J. R., Galli, G., Laus, M., Ober, C. K. and Hall, E., *Liquid Crystals*, 1993, **13**, 233.
10. Zentel, R. and Wu, J., *Makromolekular Chemistry*, 1986, **187**, 1727.
11. Fabre, P. and Veyssie, M., *Molecular Crystals and Liquid Crystals*, 1987, **4**, 99.
12. Simon, G. P., Kozak, A., Williams, G. and Wetton, R. E., *Materials Forum*, 1991, **15**, 71.
13. Mulligan, D. R., Imrie, C. T. and Larcey, P., *J. Material Science*, 1996, **31**, 1985.
14. Craig, A. A. and Imrie, C. T., *Journal of Materials Chemistry*, 1994, **4**, 1705.
15. Stewart, D. and Imrie, C. T., *Polymer*, 1996, **37**, 3419.
16. Attard, G. S., Garnett, S., Hickman, C. G., Imrie, C. T. and Taylor, L., *Liquid Crystals*, 1990, **7**, 495.
17. Nakano, T., Hasegawa, T. and Okamoto, Y., *Macromolecules*, 1993, **26**, 5494.
18. Shannon, P. J., *Macromolecules*, 1983, **16**, 1677.
19. Imrie, C. T., Karasz, F. E. and Attard, G. S., *Journal of Macromolecular Science—Pure and Applied Chemistry*, 1994, **A31**, 1221.
20. Laus, M. and Ferri, D., *Journal of Polymer Science, Polymer Physics Edition*, 1996, **34**, 1085.
21. Zentel, R., Strobl, G. R. and Ringsdorf, H., *Macromolecules*, 1985, **18**, 960.